

Unique Properties of Primary Cosmic Rays Measured by the Alpha Magnetic Spectrometer

Qi Yan,^{a,*} Vitaly Choutko,^b Yuxin Cui,^{ac} Shoudong Luo^c and Yihan Zhang^c

^a*Institute of High Energy Physics (IHEP), Chinese Academy of Sciences, Beijing 100049, China*

^b*Massachusetts Institute of Technology (MIT), Cambridge, MA 02139, USA*

^c*China Center of Advanced Science and Technology, Beijing 100190, China*

E-mail: qyan@ihep.ac.cn

We present high statistics measurements of primary cosmic rays Protons, Helium, Carbon, Oxygen, Neon, Magnesium, Silicon, Sulfur, Iron, and Nickel latest results from the Alpha Magnetic Spectrometer. The data shows that to high degree of accuracy there are only two classes of primary cosmic ray elements for nuclei with $Z \geq 2$.

42nd International Conference on High Energy Physics (ICHEP2024)
18-24 July 2024
Prague, Czech Republic

*Speaker

1. Introduction

Primary cosmic rays, such as p, He, C, O, Ne, Mg, Si, S, Fe, and Ni are mainly produced and accelerated at astrophysical sources. Precise knowledge of the primary cosmic ray spectra carry information about the sources, acceleration, and propagation processes of cosmic rays in the Galaxy.

The Alpha Magnetic Spectrometer (AMS) is a unique large acceptance, long duration magnetic spectrometer in space, operating aboard the International Space Station at an altitude of 410 km. The primary physics objectives of AMS include measuring energy spectra of cosmic-ray charged particles, nuclei, antiparticles, antinuclei, and gamma-rays to understand Dark Matter, antimatter, and the origin of cosmic rays, as well as to explore new physics phenomena.

In this paper, we report the latest AMS measurements of primary cosmic ray fluxes of p, He, C, O, Ne, Mg, Si, S, Fe, and Ni, in the rigidity range from 2 GV to 3 TV (from 1 GV to 1.8 TV for p). These measurements are based on the data collected by AMS during the first 11 years (from May 19, 2011 to Nov 11, 2022) of operation.

2. AMS Detector

The layout of the AMS detector is shown in Fig. 1. The key elements for the measurements in this paper are the permanent magnet, the nine layers, $L1-L9$, of silicon tracker [1–3] and the four planes of time of flight TOF scintillation counters [4]. The spatial resolution in each tracker layer in the bending direction is $\sim 10 \mu\text{m}$ for $Z = 1$ and $5 - 8 \mu\text{m}$ for $2 \leq Z \leq 28$ [2]. Together, the tracker and the magnet measure the rigidity R of charged cosmic rays, with a maximum detectable rigidity of 2 TV for $Z = 1$ and 3 – 3.7 TV for $2 \leq Z \leq 28$ over the 3 m lever arm from $L1$ to $L9$. Two planes of TOF counters are located above $L2$ and two planes are located below the magnet to determine the velocity ($\beta = v/c$) of passing particle. The overall velocity resolution of TOF, $\Delta(1/\beta)$, has been measured to be 4% for $Z = 1$ and 1 – 2% for $Z \geq 2$ particles. Further information on the AMS layout and performance is detailed in Ref. [5].

3. Data Analysis

The isotropic flux Φ_i in the i th rigidity bin ($R_i, R_i + \Delta R_i$) is given by

$$\Phi_i = \frac{N_i}{A_i \epsilon_i T_i \Delta R_i}, \quad (1)$$

where N_i is the number of events after background subtraction and correction for bin-to-bin migration due to finite tracker rigidity resolution, A_i is the effective acceptance, ϵ_i is the measured trigger efficiency, T_i is the collection time (which increases with rigidity due to the geomagnetic field, reaching 2.4×10^8 s above 30 GV), and ΔR_i is the rigidity bin width chosen according to the rigidity resolution and available statistics.

To accurately measure the fluxes of cosmic ray nuclei, the knowledge of nuclear interaction cross sections with the AMS material for effective acceptance A_i determination is important. The survival probabilities of nuclei ($Z \geq 2$) due to interactions in the materials were measured using cosmic ray data collected by AMS [6]. Through this study, the systematic error on nuclei fluxes measured by AMS due to uncertainties in the nuclear interactions is reduced at the percent level over the entire rigidity range. The detailed descriptions of data analysis can be found in Ref. [5, 7–12].

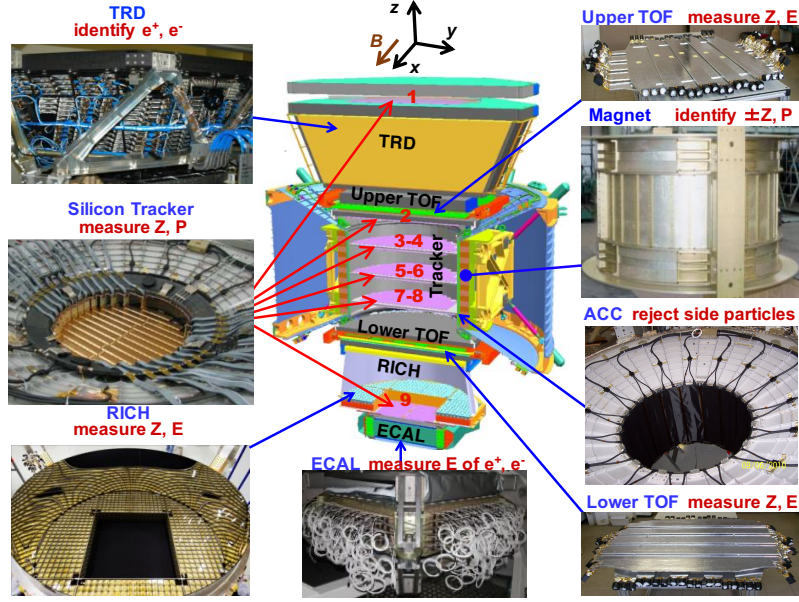


Figure 1: The AMS detector and its main components.

4. Results

p and He— Protons and helium are the most abundant charged particles in cosmic rays. Figure 2 a) and b) shows the latest AMS proton and helium fluxes as a function of kinetic energy per nucleon E_k , together with other measurements. The AMS measurements are based on 1.5 billion protons and 208 million helium nuclei. The total error is $\sim 1\%$ for proton flux and $\sim 1.5\%$ for helium flux at 50 GeV/n. Both spectra exhibit significant hardening at high energy. The proton-to-helium flux ratio as a function of kinetic energy per nucleon, together with other measurements, is shown in Fig. 2 e).

C and O— Carbon, and oxygen are among the most abundant nuclei in cosmic rays after helium. Figure 2 c) and d) shows the latest AMS carbon and oxygen fluxes as a function of kinetic energy per nucleon, compared with results from previous experiments. The total error is $\sim 3\%$ at 50 GeV/n for both the carbon and oxygen fluxes. As seen, the AMS measurements of the carbon and oxygen fluxes at high energies are very different from previous measurements, being about 20 – 40% higher above 10 GeV/n. Figure 2 f) shows the latest AMS results for the helium, carbon, and oxygen spectra. As seen, above 60 GV, all three spectra exhibit identical rigidity dependence. In particular, they all deviate from a single power law and harden progressively at a rigidity of ~ 200 GV.

Ne, Mg, Si, and S— Differences in the flux rigidity dependence of Ne, Mg, Si, and S compared to He, C, and O provide new insights into the origin and propagation of cosmic rays. The latest AMS measurements of the Ne, Mg, Si, and S fluxes, based on 2.9 million Ne, 3.5 million Mg, 2.6 million Si, and 0.47 million S nuclei, together with other measurements, are shown in Fig. 3 a) b) c) and d). The total errors is $\sim 5\%$ at 50 GeV/n for each flux. Figure 3 f) shows the rigidity dependence of the latest AMS Ne, Mg, Si, and S fluxes compared to that of the He, C, and O fluxes. As seen, above 86.5 GV, the rigidity dependences of Ne, Mg, Si, and S fluxes are identical, but distinctly

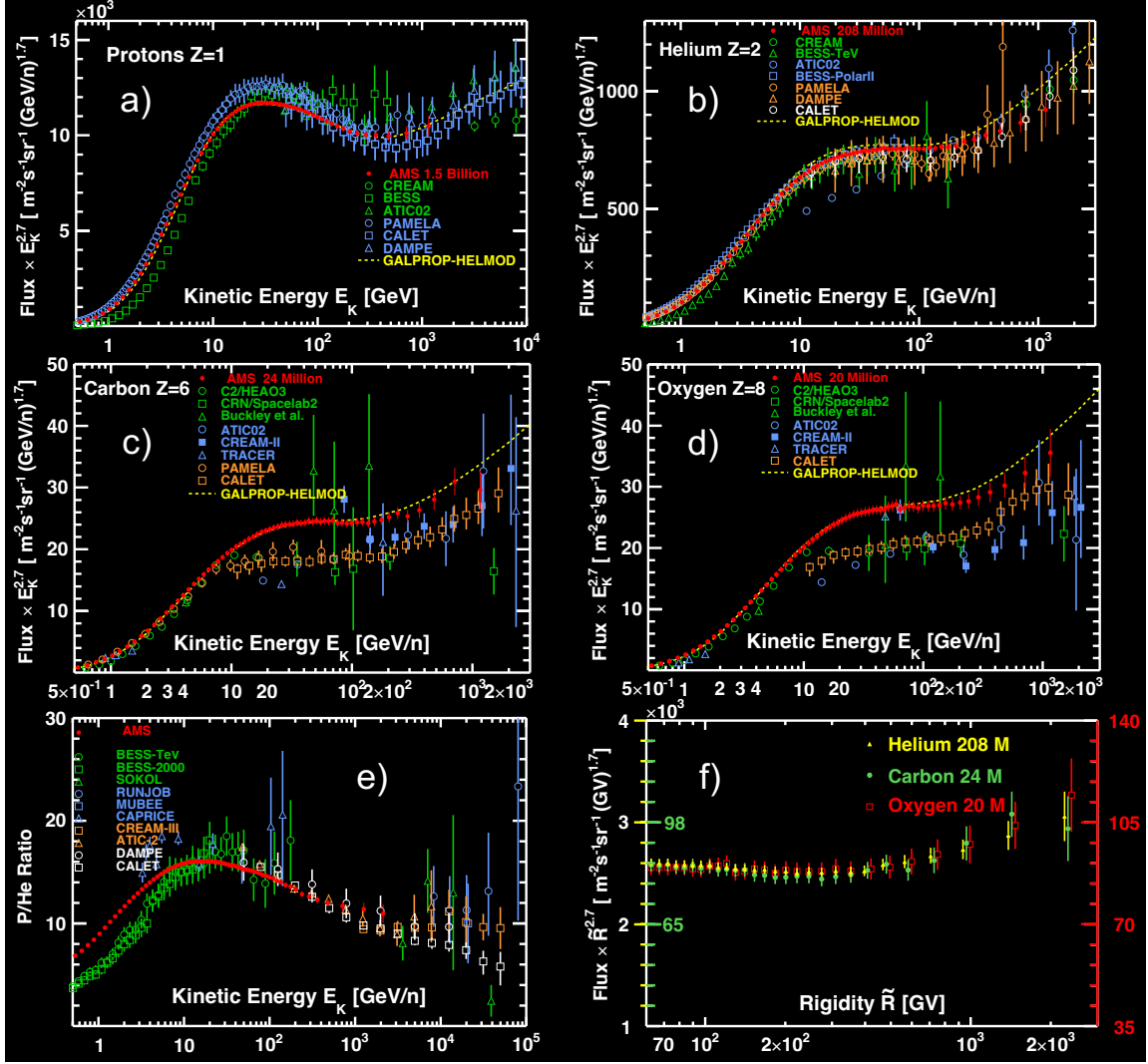


Figure 2: The AMS fluxes of a) protons, b) helium, c) carbon, and d) oxygen as a function of kinetic energy per nucleon E_K multiplied by $E_K^{2.7}$ together with other measurements. e) The AMS proton-to-helium flux ratio as a function of kinetic energy per nucleon, together with other measurements. f) The latest AMS results for the helium, carbon, and oxygen spectra above 60 GV.

different from the rigidity dependences of He, C, and O fluxes. This shows that the Ne-Mg-Si-S and He-C-O are two different classes of primary cosmic rays.

Fe and Ni—Iron and nickel are heavy nuclei beyond silicon. The rigidity dependence of the iron flux and nickel flux compared with that of lower-charge primary cosmic rays He-C-O and Ne-Mg-Si-S provide a comprehensive understanding of primary cosmic rays. Figure 3 e) shows the latest AMS iron flux based 0.9 million events as a function of kinetic energy per nucleon together with the results of previous experiments. The total error is $\sim 4\%$ at 50 GeV/n. Figure 3 f) shows the latest AMS fluxes of Fe together with He, C, O, Ne, Mg, Si, and S above 80.5 GV. As seen, the rigidity dependence of Fe flux is identical to the rigidity dependence of He, C, and O, which is different from the rigidity dependence of Ne, Mg, Si, and S. This shows that Fe belongs to the

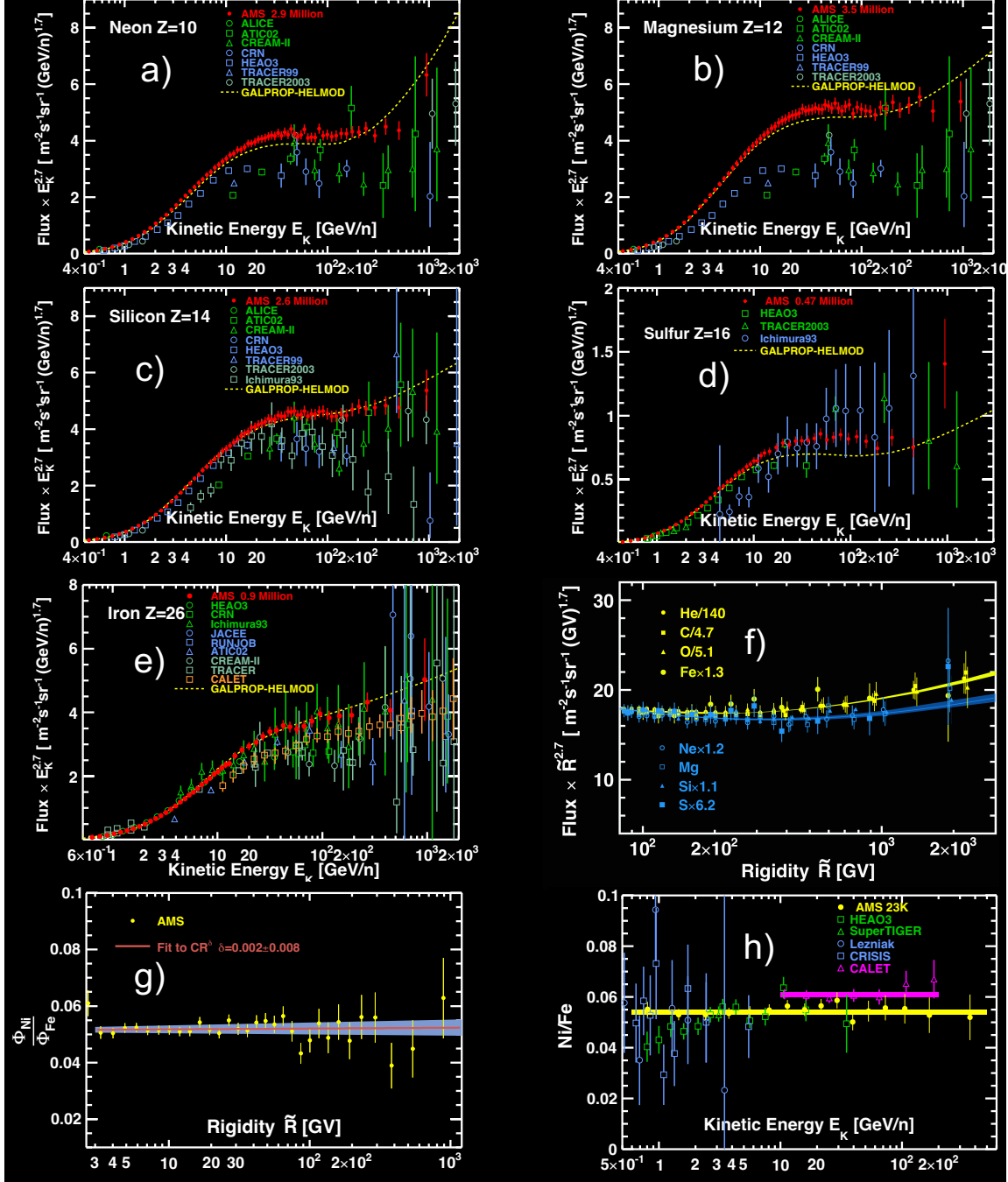


Figure 3: The AMS fluxes of a) Ne, b) Mg, c) Si, d) S, and e) Fe as a function of kinetic energy per nucleon E_K multiplied by $E_K^{2.7}$ together with other measurements. f) The rigidity dependences of the fluxes of He, C, O, Ne, Mg, Si, S, and Fe above 80.5 GV. The AMS Ni-to-Fe flux ratio g) as a function of rigidity and h) as a function of kinetic energy per nucleon together with other measurements.

same class as He, C, and O, which is different from the Ne-Mg-Si-S class of primary cosmic rays.

Figure 3 g) shows the Ni/Fe fluxes ratio fitted with a power law CR^δ above 3 GV. The fit yields $\delta = -0.002 \pm 0.008$ with $\chi^2/d.o.f = 20/29$. This shows that Ni and Fe belong to the same class of primary cosmic rays. Figure 3 h) shows the AMS Ni/Fe flux ratio compared with other measurements. As seen, the AMS result differs from the HEAO result below 2.5 GeV/n and the CALET result above 10 GeV/n.

5. Conclusions

The latest AMS results on primary cosmic ray p, He, C, O, Ne, Mg, Si, S, Fe, and Ni from 2 GV to 3 TV (from 1 GV to 1.8 TV for p) has been presented. The primary cosmic rays He-C-O-Fe-Ni and Ne-Mg-Si-S belong to two different classes of cosmic rays. Future high precision AMS measurements of all cosmic rays will continuously provide unique insight into understanding of the cosmic rays.

Acknowledgements

We acknowledge the support from Experimental Physics Division, IHEP. We are grateful for the support of Chinese Academy of Sciences. This work is supported in part by the National Natural Science Foundation of China under grant No. 12342502.

References

- [1] Q. Yan and V. Choutko, *Eur. Phys. J. C* **83** (2023) 245.
- [2] G. Ambrosi., V. Choutko, C. Delgado, A. Oliva, Q. Yan, and Y. Li, *Nucl. Instrum. Methods Phys. Res. A* **869** (2017) 29.
- [3] Y. Jia, Q. Yan, V. Choutko, H. Liu, and A. Oliva, *Nucl. Instrum. Methods Phys. Res. A* **972** (2020) 164169.
- [4] V. Bindi et al., *Nucl. Instrum. Methods Phys. Res. A* **743** (2014) 22.
- [5] M. Aguilar et al., *Phys. Rep.* **894** (2021) 1.
- [6] Q. Yan, V. Choutko, A. Oliva, and M. Paniccia, *Nucl. Phys. A* **996** (2020) 121712.
- [7] M. Aguilar et al., *Phys. Rev. Lett.* **114** (2015) 171103.
- [8] M. Aguilar et al., *Phys. Rev. Lett.* **115** (2015) 211101.
- [9] M. Aguilar et al., *Phys. Rev. Lett.* **119** (2017) 251101.
- [10] M. Aguilar et al., *Phys. Rev. Lett.* **124** (2020) 211102.
- [11] M. Aguilar et al., *Phys. Rev. Lett.* **126** (2021) 041104.
- [12] M. Aguilar et al., *Phys. Rev. Lett.* **130** (2023) 211002.